DALTON
FULL PAPER

Spectroelectrochemical studies and excited-state resonance-Raman spectroscopy of some mononuclear rhenium(I) polypyridyl bridging ligand complexes. Crystal structure determination of tricarbonyl-chloro[2,3-di(2-pyridyl)quinoxaline]rhenium(I)

Mark R. Waterland,[a] Timothy J. Simpson,[a] Keith C. Gordon *,[a] and Anthony K. Burrell *,[b]

[a] *Department of Chemistry, University of Otago, PO Box 56, Dunedin, New Zealand*
[b] *Department of Chemistry, Massey University, Private Bag 11122, Palmerston North, New Zealand*

A number of mononuclear rhenium(I) complexes have been prepared and their physical properties and excited-state and spectroelectrochemical resonance-Raman spectra studied. These compounds have the general formula $[Re(CO)_3Cl(L)]$, where L can be 2,3-di(2-pyridyl)quinoxaline (dpq), 2-(2-pyridyl)quinoxaline (pq) or 5-methyl-2,3-di(2-pyridyl)quinoxaline (mdpq). The structure of [Re(CO)Cl(dpq)] was determined by single-crystal X-ray diffraction. The NMR data for complexes with dpq and mdpq suggest the unbound pyridyl is shielding protons on the bound pyridyl moiety. The resonance-Raman spectra of the reduced complexes show some polarisation of electron density towards the bound pyridyl ring. The excited states have very similar spectral features to those of the reduced complexes. This suggests that electrochemically prepared redox states model the metal-to-ligand charge-transfer state well, for these systems.

The photophysical and electrochemical properties of d^6 metal polypyridyl complexes are of interest because of their use in solar energy conversion schemes and molecular devices.[1]

We have examined a series of mononuclear rhenium(I) complexes in which the ligands are a variation on the commonly used bridging ligand 2,3-bis(2-pyridyl)quinoxaline, dpq. We have undertaken this study with three aims in mind.

(1) We have found that binuclear rhenium(I) complexes, with dpq bridging ligands and related systems with substituents at the quinoxaline ring, show similar spectral signatures when reduced.[2] This implies the reducing electron occupies a similar molecular orbital (MO) in each case and that the electron is localised on the pyridyl ring systems. The mononuclear rhenium(I) complexes offer an opportunity to test if this localisation is extended to smaller ligand systems bound to a single $Re(CO)_3Cl$ unit. In the case of the 2-(2-pyridyl)quinoxaline (pq) complex only one pyridyl unit is present. The extent of the MO occupied by the reducing electron has implications as to the ability of the bridging ligand to facilitate electronic communication.[3]

(2) Ruthenium(II) diimine complexes with polypyridyl bridging ligands similar to dpq are of considerable interest as building blocks in photoactive supramolecular assemblies.[4] The excited-state chemistry of such complexes is dominated by metal-to-ligand charge-transfer (MLCT) excited states, in which the metal is formally oxidised and the ligand reduced. The spectroelectrochemistry of these systems can offer spectral signatures for each part of this excitation. The oxidised complex mimics the formal metal oxidation and the reduction of the complex mimics the radical anion formation at the lowest-energy ligand site, for these systems the bridging ligand L.

However attempts to measure the resonance-Raman spectra of radical anion species in $[Ru(bpy)_2L]^{2+}$ (bpy = 2,2′-bipyridine) have been frustrated by the strong scattering observed from the bpy ligands through the Ru→bpy MLCT chromophore.[5] The rhenium(I) complexes do not possess visible chromophores based on the spectator CO and Cl ligands. Hence the resonance-Raman spectra of the reduced complexes should provide the desired spectral signatures for the L radical anions.

(3) We have used pulsed laser excitation to measure the resonance-Raman spectra of the excited state of $[Re(CO)_3Cl(dpq)]$ and $[Re(CO)_3Cl(mdpq)]$ [mdpq = 5-methyl-2,3-bis(2-pyridyl)quinoxaline]. This confirms that the redox state, as formed in the electrochemical studies, and the excited state have the same spectral signature and thus similar structure.

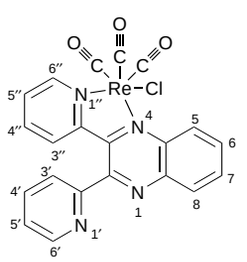

$[Re(CO)_3Cl(dpq)]$

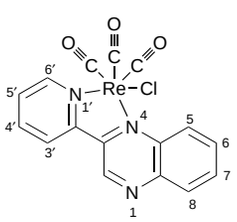

$[Re(CO)_3Cl(pq)]$

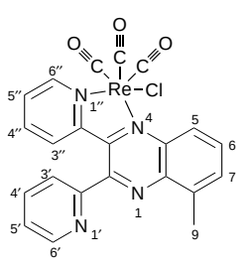

$[Re(CO)_3Cl(mdpq)]$

Experimental

Synthesis

The compounds dpq, mdpq and pq were synthesized by literature methods.[6,7] Mononuclear rhenium(I) complexes of them were prepared by addition of 1 mmol of ligand to an equimolar amount of $[Re(CO)_5Cl]$ in methanol (100 cm^3) under reflux conditions and a nitrogen gas atmosphere, for 18 h. The resulting red solution was filtered while hot to remove impurities. Upon cooling, the desired complex precipitated and was isolated by filtration.

Table 1 Electronic absorption data for ligands and complexes in CH_2Cl_2 at room temperature

Compound	λ_{max}/nm (10^{-3} ε/M^{-1} cm^{-1})				
dpq	246 (32.5)	269 (18.6)	334 (9.5)		
pq	253 (14.5)	275 (9.5)	334 (6.5)		
mdpq	253 (27.4)	275 (22)	335 (7.6)		
1		260 (18.2)		373 (7.8)	448 (2.6)
2	253 (24.9)	274 (18.5)	353 (13.1)	370 (16.3)	449 (3.4)
3		280 (29.8)		368 (11.3)	439 (4.3)

dpq: δ_H(300 MHz, solvent $CDCl_3$, standard $SiMe_4$) 8.38 (d, 2 H, $H^{6'}$, $H^{6''}$), 8.23 (q, 2 H, H^5, H^8), 7.97 (d, 2 H, $H^{3'}$, $H^{3''}$), 7.81 (m, 4 H, $H^{4'}$, $H^{4''}$, H^6, H^7) and 7.23 (m, 2 H, $H^{5'}$, $H^{5''}$) (Found: C, 75.8; H, 4.0; N, 19.9. Calc.: C, 76.1; H, 4.2; N, 19.7%); yield 61%.

pq: δ_H(300 MHz, $CDCl_3$, $SiMe_4$) 9.97 (s, 1 H, H^3), 8.79 (dd, 1 H, $H^{6'}$), 8.61 (dd, 1 H, $H^{3'}$), 8.17 (m, 2 H, H^5, H^6), 7.90 (td, 1 H, $H^{4'}$), 7.80 (m, 2 H, H^7, H^8) and 7.41 (td, 1 H, $H^{5'}$) (Found: C, 75.42; H, 4.57; N, 20.51. Calc.: C, 75.33; H, 4.38; N, 20.28%); yield 31%.

mdpq: δ_H(300 MHz, $CDCl_3$, $SiMe_4$) 8.3 (dd, 2 H, $H^{6'}$, $H^{6''}$), 8.14 (d, 1 H, $H^{3'}$), 8.10 (dd, 1 H, H^6), 7.96 (d, 1 H, $H^{3''}$), 7.82 (m, 2 H, $H^{4'}$, $H^{4''}$), 7.7 (m, 2 H, H^5, H^7), 7.23 (m, 2 H, $H^{5'}$, $H^{5''}$) and 2.88 (s, 1 H, H^9) (Found: C, 64.47; H, 4.01; N, 16.06. Calc. for mdpq·$3H_2O$: C, 64.74; H, 4.01; N, 15.91%); yield 81%.

[$Re(CO)_3Cl$(dpq)] **1**: δ_H(300 MHz, $CDCl_3$, $SiMe_4$) 9.16 (d, 1 H, $H^{6''}$), 8.85 (m, 2 H, $H^{6'}$, H^5), 8.32 (m, 1 H, H^8), 8.01 (m, 3 H, $H^{3'}$, H^6, H^7), 7.89 (td, 1 H, $H^{4''}$), 7.69 (td, 1 H, $H^{4'}$), 7.49 (m, 2 H, $H^{5'}$, $H^{5''}$) and 7.26 (d, 1 H, $H^{3''}$) (Found: C, 42.48; H, 2.05; N, 9.34. Calc.: C, 42.75; H, 2.05; N. 9.50%); yield 47%.

[$Re(CO)_3Cl$(pq)] **2**: δ_H(300 MHz, $CDCl_3$, $SiMe_4$) 9.75 (s, 1 H, H^3), 9.23 (d, 1 H, $H^{6'}$), 8.86 (dd, 1 H, H^8), 8.57 (d, 1 H, H^5), 8.26 (m, 2 H, $H^{4'}$, H^6), 8.08 (m, 2 H, $H^{3'}$, H^7) and 7.70 (m, 1 H, $H^{5'}$) (Found: C, 37.40; H, 1.66; N, 8.39. Calc.: C, 37.47; H, 1.77; N, 8.19%); yield 77%.

[$Re(CO)_3Cl$(mdpq)] **3**: δ_H(300 MHz, $CDCl_3$, $SiMe_4$) 9.13 (d, 1 H, $H^{6'}$), 8.71 (s, 1 H, H^9), 8.68 (m, 1 H, $H^{6''}$), 8.15 (d, 1 H, $H^{3''}$), 8.01 (td, 1 H, $H^{4''}$), 7.91 (m, 2 H, H^7, H^8) and 7.71 (td, 1 H, $H^{4'}$), 7.51 (m, 2 H, $H^{5'}$, $H^{5''}$), 7.25 (d, 1 H, $H^{3'}$) and 2.88 (s, 3 H, H^9) (Found: C, 43.76; H, 1.98; N, 9.61. Calc.: C, 43.75; H, 2.34; N, 9.28%); yield 48%.

Physical measurements

Infrared absorption spectra were recorded on a Bio-Rad FTS-60 FTIR spectrometer, electronic absorption spectra on a Perkin-Elmer Lambda-19 spectrophotometer. Cyclic voltammograms were obtained from nitrogen-degassed dichloromethane solutions containing 0.1 M NBu_4ClO_4 as supporting electrolyte and complex at 1 mM concentration. The measurements were carried out using an EG & G PAR 273A potentiostat, with model 270 software, referenced to a saturated calomel electrode (SCE). The NMR spectra were recorded using a Varian 200 MHz instrument. Resonance-Raman measurements used a Spectra-Physics model 166 argon-ion laser to generate Raman scattering. Scattering was collected in a 135° back-scattering geometry and imaged using a two-lens arrangement [8] into a Spex 750M spectrograph. Raman photons were detected using a Princeton Instruments liquid-nitrogen-cooled 1152-EUV charge-coupled device. Rayleigh and Mie scattering from the sample was attenuated using a Notch filter (Kaiser Optical Systems Inc.) of appropriate wavelength. Silver sols were prepared by a standard method.[9] Spectroelectrochemical Raman and electronic absorption measurements were facilitated with a thin-layer electrochemical cell.[10]

For the excited-state resonance-Raman measurements, 448.3 nm pulsed excitation was employed. This was generated by stimulated Raman scattering [11] through acetonitrile, contained in a 10 cm cell, using the 354.7 nm third harmonic of the Nd:YAG pulsed laser. It was found that with 50 mJ per pulse of 354.7 nm light, 3.5 mJ per pulse of 448.3 nm was obtained. The pulse energy of the 448.3 nm beam was attenuated by lowering the 354.7 nm pump energy.

Crystallography

Single crystals of complex **1** were grown by the slow diffusion of diethyl ether into a solution of the complex dissolved in dichloromethane. A red rod-shaped crystal with approximate dimensions 0.35 × 0.81 × 0.34 mm was secured to the end of a glass fibre with cyanoacrylate glue. Crystallographic data are summarised in Table 4. All other relevant data are available as supporting material. Intensity data were collected using an Enraf-Nonius CAD-4 diffractometer (293 K, Mo-Kα X-radiation, graphite monochromator, λ = 0.710 73 Å) in the range $4 \leqslant 2\theta \leqslant 64$ by the θ–2θ scan mode with index ranges $-11 \leqslant h \leqslant 10$, $0 \leqslant k \leqslant 30$, $0 \leqslant l \leqslant 19$. A total of 7131 reflections were collected, of which 6884 were unique (R_{int} = 0.0097). The data were corrected for Lorentz-polarisation, and X-ray absorption effects, the last by an empirical method based on azimuthal scan data (T_{max} : T_{min} = 0.812 : 0.514).[12] No correction for extinction was applied. Scattering factors are included in SHELXL 93.[13] Systematic monitoring of three check reflections showed no systematic crystal decay and no correction was applied. The position of the Re atom was determined from a Patterson synthesis. Calculations were carried out using an IBM compatible 486 computer and SHELXL 93. The remaining non-hydrogen atoms were located by application of a series alternating least-squares cycles and Fourier-difference maps. All non-hydrogen atoms were refined with anisotropic displacement parameters. Hydrogen atoms were included in the structure factor calculations at idealised positions but were not subsequently refined. Final least-squares refinement of 271 parameters resulted in residuals $R(F_o)$ of 0.0308 and $R'(F_o^2)$ of 0.0745 [$F_o > 4\sigma(F_o)$]. After convergence the quality of fit on F_o^2 was 1.005 and the highest peak in the final difference map was 1.275 e $Å^{-3}$ located close to the Re atom. Selected bond lengths and angles are given in Table 5.

CCDC reference number 186/753.

Results

The infrared absorption spectra of complexes **1**–**3** in CH_2Cl_2 solution show three bands in the carbonyl stretching region. For all complexes these lie at 2025, 1925 and 1905 cm^{-1}. This pattern corresponds to 3 CO units in a *fac* isomer arrangement. They are assigned as the A′(1), A″ and A′(2) vibrations respectively.[14] The wavenumbers of the CO stretches are very sensitive to the d_π electron density (oxidation state) of the rhenium centre.[15] The constancy of the wavenumbers indicates the ligands have an equivalent perturbation on the metal centre.

Electronic absorption data for complexes are presented in Table 1. The three ligands show $\pi \longrightarrow \pi^*$ transitions at about 250, 275 and 334 nm. These are shifted upon complexation to the $Re(CO)_3Cl$ unit. Each complex has two MLCT bands at *ca.* 370 and 440 nm.

Electrochemical data are presented in Table 2. Oxidation waves are irreversible for all three complexes; in these cases the data reported are for the anodic peak in the cyclic voltam-

Table 2 Electrochemical data for complexes in CH_2Cl_2 at room temperature

Compound	E_{pa}[a]/V Oxidation	$E^{\circ\prime}$[b]/V *vs.* SCE Reduction
1	1.62	−0.75
2	1.59	−0.75
3	1.63	−0.81

[a] The oxidations are irreversible and the values given are for the anodic peak in the cyclic voltammogram. [b] $E^{\circ\prime} = \frac{1}{2}(E_{pa} + E_{pc})$, the value between the anodic and cathodic peaks of the cyclic voltammogram.

mogram. This is common for $[Re(CO)_3Cl(L)]$ complexes and is assigned as a metal-centred oxidation from rhenium-(I) to -(II).[16] The first reduction for all three complexes is reversible, in that it shows a peak separation between anodic and cathodic peaks close to 60 mV and in the spectroelectrochemical experiments it is possible completely to regenerate the starting material. The reduction is assigned as ligand-centred, based on comparison with similar complexes.[17]

The resonance-Raman spectra of the complexes and the corresponding reduced species, generated using 488 nm excitation, are shown in Fig. 1. Band positions are in Table 3. All bands are polarised, consistent with an A-term scattering mechanism.[18] All the complexes emit in CH_2Cl_2 solution making resonance-Raman spectra noisy, particularly in the higher-wavenumber region.

An excitation wavelength of 488 nm is resonant with the MLCT transitions of each of the complexes. The strong enhancement of the CO vibration is consistent with this. The MLCT excited state formally oxidises $Re^{I} \longrightarrow Re^{II}$ and the CO bond length and wavenumber position are perturbed by this. Other than the carbonyl stretch there are a number of ligand-based vibrational modes which are enhanced in the resonance-Raman spectra (Fig. 1, Table 3). Most of these features lie between 1600 and 600 cm^{-1}. A number of the ligand modes are strongly enhanced; these lie at 1476 and 1326 cm^{-1} for **1** and 1470 and 1335 cm^{-1} for **3**. For **2** a strong band is observed at 1483 cm^{-1} with a weaker feature at 1339 cm^{-1}.

The band positions observed in the Raman spectra of the ligands are shown in Table 3. The strong luminescence of pq and mdpq required their Raman spectra to be measured using a silver sol to quench emission and increase signal intensity, through the surface-enhanced Raman scattering (SERS) effect.[19] The spectra of dpq and mdpq are similar with strong bands at 1390 and in the 1470 cm^{-1} region and with weak features in the 1600–1550 cm^{-1} region. The SERS spectrum of pq shows strong features at 1371 cm^{-1} with bands at 1476, 1551 and 1576 cm^{-1}.

Electronic absorption spectra of the reduced complexes are shown in Fig. 2. Reduction of **1** leads to bleaching of the 373 nm MLCT band and a new band appears at 390–400 nm; $\mathbf{1}^-$ absorbs across much of the visible region and the absorbance at 448 nm is barely changed upon reduction. A similar pattern of changes is observed for **2** and **3**. In both cases a feature at 390–400 nm is present. The spectra observed in the optically transparent thin-layer electrode (OTTLE) experiments were stepped through a series of potentials across the respective reduction wave. Spectral changes observed occurred smoothly showing isosbestic points at 244, 314, 342, 390 and 429 nm for **1**, 235, 288 and 322 nm for **2** and 321, 352, 389, 421 and 489 nm for **3**.

Resonance-Raman spectra, generated at 488 nm, for the reduction products are shown in Fig. 1. Band positions for reduced complexes are presented in Table 3. The reductions of **1** and **2** are characterised by the complete bleaching of the CO band at *ca.* 2026 cm^{-1}. Therefore, the other observed features in the resonance-Raman spectra are entirely due to the reduced species; no residual parent complex is present in the irradiated volume. The situation is more complex for the reduction of **3** to

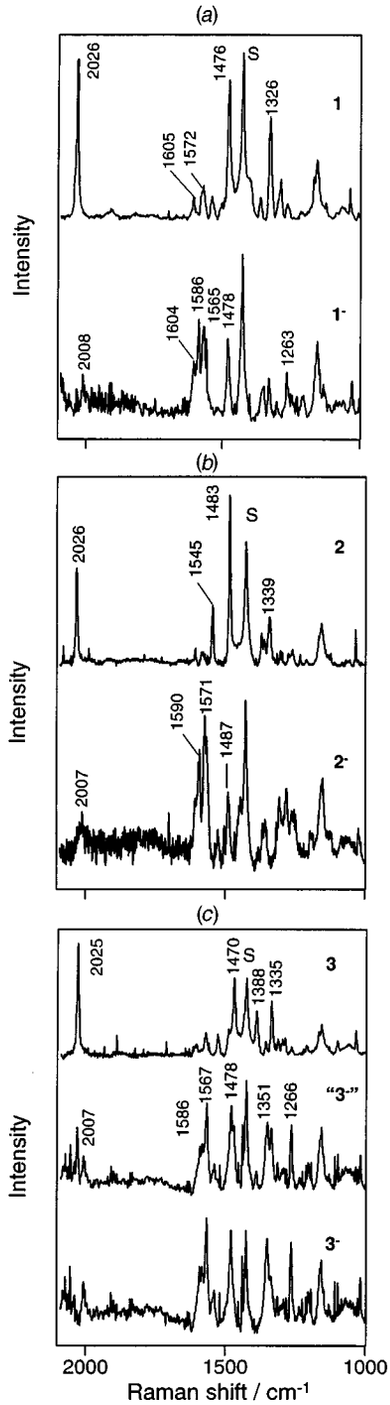

Fig. 1 Resonance-Raman spectra (λ_{exc} = 488 nm, 10 mW at sample) of 5 mM solutions of complexes in CH_2Cl_2 measured in a spectroelectrochemical cell with 0.1 M NBu_4ClO_4 supporting electrolyte: (*a*) upper trace **1**, lower trace $\mathbf{1}^-$; (*b*) upper trace **2**, lower trace $\mathbf{2}^-$; (*c*) upper trace **3**, middle trace partly reduced sample of $\mathbf{3}^-$, lower trace $\mathbf{3}^-$. S indicates solvent band

$\mathbf{3}^-$. When a reducing potential is applied to **3** new features grow in but the parent bands are not bleached. The intensity of the parent species CO band indicates about 15% residual **3** in the reduced solution. These residual ground-state features may be subtracted out of the spectrum to produce a pure reduced-species spectrum. This is shown in Fig. 1(*c*), lower trace. In each case the original parent-complex spectrum was regenerated by reoxidation of the sample. Hence, under the conditions of these experiments, the reductions were chemically reversible.

A weak CO feature is observed to lower wavenumbers for each of the reduced species. The small enhancement of this band suggests the resonant transition for the reduced species at

Table 3 Wavenumbers (cm^{-1}) of observed Raman bands for ligands, complexes and reduced species in CH_2Cl_2 solution

dpq[a]	**1**[b]	**1**$^{-}$[b]	pq[c]	**2**[b]	**2**$^{-}$[b]	mdpq[c]	**3**[b]	**3**$^{-}$[b]
	2026s	2008w		2026s	2007w		2025s	2007
1591	1605w	1604		1603w	1604 (sh)	1599w	1605w	
	1572	1586	1576	1575w	1590		1569	1586
	1530w	1565	1551	1545	1571	1533w	1525w	1567
					1560w		1487 (sh)	1542w
1475	1476s	1478	1476	1483s	1487	1472	1470s	1478
1441	1406				1444			
1398	1360	1351	1371s	1368	1361	1390s	1388s	
			1356	1357	1353		1355w	1351
1324	1326	1326	1320	1339			1335s	
					1305		1312w	
				1301w			1299w	
					1280		1286w	1266
	1261w	1263		1260w	1258		1263w	

s = Strong; w = weak, sh = shoulder. [a] λ_{exc} = 632.8 nm. [b] λ_{exc} = 488 nm, Fig. 1. [c] λ_{exc} = 457.9 nm, SERS spectrum.

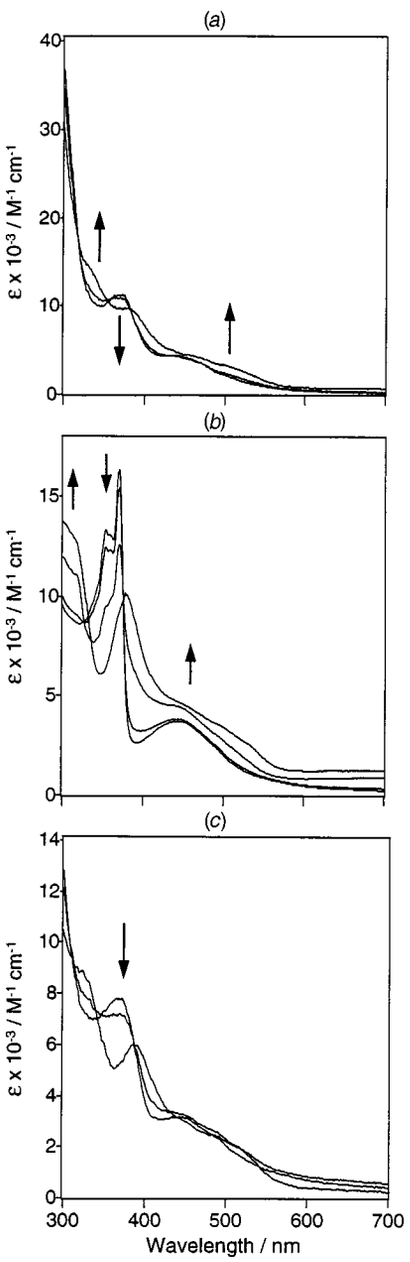

Fig. 2 Electronic absorption spectra of complexes measured in a spectroelectrochemical cell at varying potentials: changes in the electronic absorption spectrum (CH_2Cl_2 solution with 0.1 M NBu_4ClO_4 supporting electrolyte) upon electrochemical reduction (arrows indicate changes on stepping through 0.0 V to −1.2 V applied potential *versus* Ag^+–AgCl) for (*a*) **1**, (*b*) **2** and (*c*) **3**

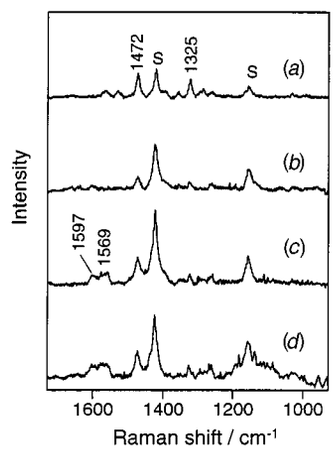

Fig. 3 Resonance-Raman spectra of complex **1**, CH_2Cl_2 solution, with: (*a*) 457.9 nm continuous-wave excitation, (*b*) 448.2 nm pulsed excitation, 0.7 mJ per pulse, (*c*) 1.0 mJ per pulse and (*d*) 1.8 mJ per pulse. Beam diameter at sample for the pulsed studies = 400 μm

488 nm is not metal-centred but probably a ligand-centred $\pi \longrightarrow \pi^*$ transition.[20]

The reduction **1** $\longrightarrow$ **1**$^{-}$ results in the following spectral changes. (1) The CO band at 2026 cm^{-1}, which is very strongly enhanced in the spectrum of **1**, is completely absent from the spectrum of **1**$^{-}$. A weak feature is observed at 2008 cm^{-1}. (2) A group of intense bands at 1604, 1586 and 1565 cm^{-1} appear when **1** is reduced. The spectrum of **1** shows a number of weak bands at 1605, 1572 and 1530 cm^{-1}. (3) A strong band at 1476 cm^{-1} for **1** is slightly shifted upon reduction to 1478 cm^{-1}. This band retains intensity in the spectrum of **1**$^{-}$. (4) A number of weak features are also present at 1351, 1326 and 1263 cm^{-1}. The 1326 cm^{-1} band is a strong feature of **1**.

The resonance-Raman spectrum of complex **2**$^{-}$ [Fig. 1(*b*)] shows features at 2007 cm^{-1}, in the 1550 to 1610 cm^{-1} region, as well as some bands in the 1240 to 1310 cm^{-1} region. The strongly enhanced ligand vibrational transition at 1483 cm^{-1} of **2** appears shifted to 1487 cm^{-1} for **2**$^{-}$.

The resonance-Raman spectrum of complex **3**$^{-}$ [Fig. 1(*c*), lower trace] is similar to that of **1**$^{-}$. A weak CO band is observed at 2007 cm^{-1} and a group of intense bands appear at 1586 and 1567 cm^{-1}. The spectrum of **3** has a strong band at 1470 cm^{-1} which shifts to 1478 cm^{-1} upon reduction. Features appear at 1351 and 1266 cm^{-1}. All of these features are wavenumber coincident with those of **1**$^{-}$.

The resonance-Raman spectra of complexes **1**–**3** were measured using pulsed excitation. With 448 nm pulses (7 ns duration) it was possible to measure the spectrum of the MLCT excited state. Figs. 3 and 4 show the spectra of **1** and **3** respectively as a function of increasing pulse energy. As the pulse

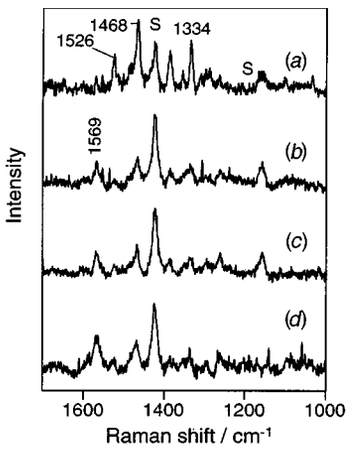

Fig. 4 Resonance-Raman spectra of complex **3**, CH_2Cl_2 solution. Details as in Fig. 3

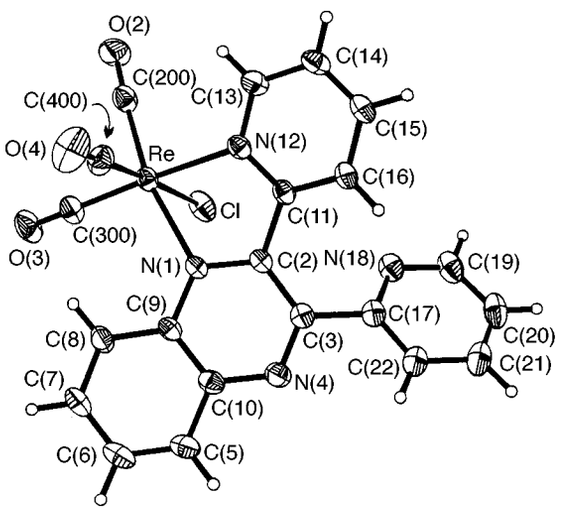

Fig. 5 An ORTEP[22] drawing of complex **1** with the atomic numbering scheme. Thermal ellipsoids are shown at the 30% probability level

energy is increased the excited-state features grow in. A plot of ln *E*, where *E* is the pulse energy, *vs.* ln *I*, where *I* is the intensity of the band, shows a gradient >1. This is indicative of an excited-state band.[21]

For complex **1** (Fig. 3) the excited-state bands appear at 1597 and 1569 cm^{-1} at the highest photon flux used. The ground-state band at 1530 cm^{-1} is completely bleached, however ground-state features at 1472 and 1325 cm^{-1} persist. This may be because they are also excited-state features.

The spectrum of complex **2** generated using 448 nm excitation was noisy and no excited-state features could be observed. That of **3** (Fig. 4) shows the growth of a band at 1569 cm^{-1} (ln *E vs.* ln *I* gradient = 1.8). The ground-state features at 1334 and 1526 cm^{-1} show much reduced intensity in the high-flux spectra.

One complication of these measurements was that the mononuclear complexes showed some decomposition with prolonged pulsed irradiation. In a typical experiment about 5–10% of the complex decomposed as measured by UV/VIS spectra. The decomposition product led to the appearance of a band at 1985 cm^{-1} (not shown in the spectra). However, ground-state resonance-Raman spectra of solutions after prolonged pulsed excitation retained the 1985 cm^{-1} band only; no other features observed in the pulsed spectra were detected in the spectra of these solutions. Therefore the features reported above are only present with pulsed excitation.

Discussion

A perspective drawing of complex **1** is depicted in Fig. 5. The

Table 4 Crystal data for complex **1**

Formula	$C_{21}H_{12}ClN_4O_3Re$
M	590
Crystal system	Monoclinic
Space group	$P2_1/c$ (no. 14)
T/°C	20
a/Å	7.4480(14)
b/Å	20.273(8)
c/Å	13.397(5)
β/°	99.83(2)
U/Å^3	1993.2(11)
Z	4
μ/mm^{-1}	6.262
D_c/g cm^{-3}	1.966
$R'(F_o^2)$	0.0745*
$R(F_o)$	0.0308

* $R'(F_o^2) = [\Sigma w(F_o^2 - F_c^2)^2/\Sigma w(F_o^2)^2]^{\frac{1}{2}}$ where $w^{-1} = [\sigma^2(F_o^2) + (aP)^2 + bP]$ $\{a = 0.0361, b = 1.4198$ and $P = [\max(F_o^2, 0) + 2F_c^2]/3\}$. The structure was refined on F_o^2 using all data; the $R(F_o)$ value is given for comparison with older refinements based on F_o with a threshold of $F > 4\sigma(F)$ and $R(F_o) = \Sigma||F_o| - |F_c||/\Sigma|F_o|$; *R* factors based on F^2 are statistically about twice as large as those based on *F*.

Table 5 Selected bond lengths (Å) and angles (°) for complex **1**

Re–C(200)	1.910(4)	N(4)–C(10)	1.364(5)
Re–C(300)	1.915(4)	N(12)–C(11)	1.335(5)
Re–C(400)	1.930(5)	N(12)–C(13)	1.353(5)
Re–N(12)	2.160(3)	N(18)–C(17)	1.337(5)
Re–N(1)	2.222(3)	N(18)–C(19)	1.339(5)
Re–Cl	2.462(1)	C(200)–O(2)	1.141(5)
N(1)–C(2)	1.336(4)	C(300)–O(3)	1.151(5)
N(1)–C(9)	1.384(4)	C(400)–O(4)	1.105(6)
N(4)–C(3)	1.315(5)		
C(200)–Re–C(300)	87.0(2)	C(400)–Re–N(1)	94.3(2)
C(200)–Re–C(400)	91.2(2)	N(12)–Re–N(1)	73.7(1)
C(300)–Re–C(400)	91.7(2)	C(200)–Re–Cl	92.4(2)
C(200)–Re–N(12)	94.6(1)	C(300)–Re–Cl	89.2(2)
C(300)–Re–N(12)	176.2(2)	C(400)–Re–Cl	176.3(1)
C(400)–Re–N(12)	91.7(2)	N(12)–Re–Cl	87.33(9)
C(200)–Re–N(1)	167.1(1)	N(1)–Re–Cl	81.99(8)
C(300)–Re–N(1)	104.5(1)		

co-ordination geometry at the Re atom is a distorted octahedron with three carbonyl ligands arranged in the facial fashion. The N(12)–Re–N(1) angle being 73.7(1)° is significantly smaller than 90°, resulting from the small bite angle of the polypyridyl ligand. The rhenium–carbonyl bond lengths do not show any significant differences [1.910(4), 1.915(4) and 1.930(5) Å] but are consistent with those observed in similar complexes.[23] The two Re–N bonds although chemically distinct are similar and the distances are within the range expected for such complexes.[23] The ligand is distorted from planarity by steric interactions between the pyridyl rings. The free pyridyl ligand [C(17)–N(18)–C(19)–C(20)–C(21)–C(22)] is rotated, at an angle of 53.0(1)°, with respect to the co-ordinated pyridyl ligand [C(11)–N(12)–C(13)–C(14)–C(15)–C(16)] to minimise the steric interactions with the hydrogen atom on C(16). The co-ordinated pyridine is slightly twisted [15.3(4)°] with respect to the pyrazine. In contrast the free pyridine is significantly more twisted at 33.1(4)°, with respect to the pyrazine. Interestingly, the distortion of the free pyridine, with respect to the co-ordinated portion of the ligand, in $[Ru(bpy)_2(dpq)]^{2+}$ is much greater than that observed for **1**, at 66°.[23q] As the free pyridine is distant from the site of co-ordination in all of the structurally characterised[23p–r] mononuclear complexes of dpq, and related ligands, there is no strong steric reason for significant deviations from the geometry observed in the free ligand.[23r] The significance of these distortions and the variations observed between different complexes are yet to be explained.

Electrochemical data (Table 2) show that complex **3** is signifi-

cantly more difficult to reduce than **2** or **1**, consistent with the higher energy of the MLCT transition of **3**. The reduction potentials for **1** and **2** are similar suggesting that the removal of the second pyridyl ring has little effect on the electron-accepting redox orbital involved in the reduction process. The first oxidation potentials are all irreversible, however the oxidation potential of **2** is significantly higher than for **1** or **3**.

The NMR spectrum of complex **1** in comparison to the ligand, dpq, and its binuclear analogue [{$Re(CO)_3Cl$}$_2$dpq], is complex. The chemical shifts of the 3′ and 3″ protons on going from the dpq ligand to **1** are particularly interesting. The $H^{3'}$ resonance is practically unshifted upon chelation of the $Re(CO)_3Cl$ moiety. The $H^{3''}$ resonance shifts 0.71 ppm upfield. This is a surprising finding in view of the fact that the rhenium should deshield the protons of the chelating pyridine ring.[24] For [{$Re(CO)_3Cl$}$_2$dpq] **4** the $H^{3'}$ and $H^{3''}$ resonances lie at δ 8.48. The NMR spectra of mdpq and **3** show similar shift patterns, with the $H^{3''}$ shifting upfield by 0.72 ppm and the $H^{6''}$ shifting 0.79 ppm downfield, upon chelation.[2] It is interesting that the $H^{6''}$ and $H^{3''}$ shifts for pq to **2**, where there is no unbound pyridyl ring, are significantly smaller, 0.45 and −0.54 ppm respectively. An analysis of the shift patterns on going from 2,3-dipyridylpyrazine (dpp) to [$Re(CO)_3Cl$(dpp)] carried out by Guarr and co-workers[24] reveals similar effects. Notably, the resonances of H α to the chelating N atoms (akin to $H^{6''}$ for **1**–**3**) are shifted 0.80 ppm downfield with chelation; $H^{3''}$ is shifted 0.71 ppm upfield.

The most plausible explanation for this finding is that the unbound pyridine ring is interacting with the $H^{3''}$ of the bound ring. This could occur by interaction of the N atom of the unbound ring [N(18) in Fig. 5] with $H^{3''}$ (H from C^{16} in **1**–**3**) or by ring-current effects from the unbound ring affecting $H^{3''}$. Kaizu and co-workers[25] have reported the latter effect in the NMR spectrum of $[Ru(CN)_4(bpy)]^{2-}$. They found that the resonances of the α-H were deshielded by ring currents of the CN moiety. For $[Ru(bpy)_3]^{2+}$ the resonances lie at δ 7.73, whereas for $[Ru(CN)(bpy)_4]^{2-}$ they lie at δ 9.42.

The single-crystal structure of complex **1** shows a N(4) to $H^{3'}$ distance of 2.57 Å and a N(18) to $H^{3''}$ distance of 2.46 Å. If the nitrogen is directly interacting with the hydrogen to shield it, then this effect should be very similar for $H^{3'}$ and $H^{3''}$. However, the resonances for these protons lie at δ 8.01 and 7.26, respectively. A through-space interaction from the N atoms is therefore ruled out.

If one considers the ring current of the unbound pyridyl ring as being the source of shielding of $H^{3'}$ then the crystal structure clearly shows that no shielding can occur. A cylinder projected normal to the unbound pyridyl ring does not encapsulate $H^{3''}$. This implies that the solution-phase structure is rather different from the crystal structure. The rotation of the unbound pyridyl ring out of the plane of the quinoxaline is consistent with the electrochemistry findings in which the reduction potentials for **1** and **2** are very similar.

Electronic spectra of the reduced species show absorption throughout the visible region with a band at 400 nm for each of the complexes. The long-wavelength absorptions are ligand-centred transitions involving the redox orbital and higher-lying ligand π* orbitals. The more intense band at 400 nm may be a MLCT transition. The energy of the transition is altered by the modification to the electron configuration of the ligand caused by reduction. The electronic absorption spectra for $\mathbf{1}^-$–$\mathbf{3}^-$ appear similar, however the spectrum of $\mathbf{1}^-$ differs significantly from that of $\mathbf{4}^-$. For the binuclear complex the reduced species absorbs out to 550 nm;[2] the mononuclear species clearly do not absorb to that extent in the red. Their radical anion transitions are significantly blue-shifted. This would suggest the reducing electron in the radical anion occupies an MO more extensively spread out than for the mononuclear systems.

The crystal structure determination reveals a non-planar ligand configuration. It is unlikely the pyridine and quinoxaline ring systems can be planar.[26] The crystallographic data on **1** and dpq[27] show that the C–C and C–N bond lengths are very similar in the free and bound ligand. Any shifts in wavenumber for the ligand vibrational normal modes are, therefore, primarily a consequence of changes in the reduced mass of the vibration, due to the presence of the rhenium centre. In the normal coordinate analysis of $[Ru(bpy)_3]^{2+}$ higher-wavenumber vibrations have modest contributions from the metal centre motion.[28] One can therefore interpret the spectra of the complexes in terms of the ligand moieties. Previous studies into binuclear ruthenium complexes of dpq[29] reveal that many of the features observed in the Raman spectra are quinoxaline based.

The resonance-Raman spectra of the reported complexes all possess a strong transition at *ca.* 1470 cm^{-1}. This feature also turns up in the ligand spectra and is assigned as a vibration associated with the quinoxaline ring system. Vibrational modes at 1600 to 1500 cm^{-1} are also observed for each of the three complexes. These bands are weakly enhanced in comparison to the 1470 cm^{-1} band. The spectra of **1** and **3** are almost identical in this region. The highest-frequency quinoxaline vibrational mode which is primarily C–C and C–N based is at 1575 cm^{-1}.[25] The observed bands at 1605 and 1582 cm^{-1} cannot therefore be quinoxaline based. However, 2-substituted pyridines show strong Raman features at 1620–1570, ν_{8a}, and 1580–1560 cm^{-1}, ν_{8b}.[30] We assign these high-frequency modes as pyridine-based vibrations. The other notable feature is at *ca.* 1330 cm^{-1}. At this frequency it is possible the mode is quinoxaline based or the C–C stretch of the inter-ring linkage. Inter-ring vibrations for polypyridyl ligands in metal complexes are common at this frequency[31] and we assign this band to that vibrational mode. For **1** and **3** strong bands are observed at 1326 and 1335 cm^{-1} respectively. In the case of **2** where only one inter-ring bond is present a feature at 1339 cm^{-1} is observed. If these assignments are correct then the strong enhancement of the quinoxaline mode in comparison to the pyridyl modes suggests the optical electron in the MLCT transition will occupy a MO with greater wavefunction amplitude on the quinoxaline ring system. A similar observation was made for the binuclear rhenium(I) complexes.[2]

In regard to the nature of the redox MO, a number of limiting situations are possible. It may be delocalised over the entire ligand or localised predominantly on a single ring system (the pyridyl or quinoxaline rings). Analysis of the resonance-Raman spectra of the reduced complexes with respect to each other and the related reduced binuclear complex, $\mathbf{4}^-$, offer some insight into the nature of the MO.

There are significant changes in the resonance-Raman spectra of the complexes upon reduction. Despite the reduced enhancement in the CO region it is possible to observe carbonyl bands for the reduced species. For all of the complexes the CO band is at lower frequency for the reduced species than for the ground state. This is due to the population of the π* ligand orbital which feeds electron density through the d_π orbitals to the π* MO of the carbonyl ligands. The resulting increase in antibonding character for the CO linkage results in downshift in the frequency of vibration.[32]

All three reduced complexes show strong bands at *ca.* 1590 and 1570 cm^{-1} with a weaker shoulder at *ca.* 1605 cm^{-1}. The wavenumber values for these bands correspond very closely to those for the binuclear system, $\mathbf{4}^-$, and its analogues.[2] These factors suggest that the high-wavenumber modes are predominantly pyridyl in nature. The similarity in wavenumber for the modes also suggests that the pyridyl unit has a similar structure in each of the reduced complexes. This is consistent with a redox MO localised on the pyridyl function. Furthermore, the fact that the spectrum of $\mathbf{2}^-$ is similar to that for the other two reduced complexes indicates that the pendant pyridyl ring has little effect on the redox MO.

A strong band is observed at 1478 cm^{-1} for $\mathbf{1}^-$ and $\mathbf{3}^-$; for $\mathbf{2}^-$ this lies at 1487 cm^{-1}. In the spectrum of the related $\mathbf{4}^-$ no features are observed in the 1470 cm^{-1} region. Coupled with the fact that in the parent species there is a strong quinoxaline based vibration in this region suggests that the 1478 cm^{-1} band is quinoxaline based. There are two ways in which a quinoxaline-based band may be enhanced in the spectrum of the reduced complexes. If the redox MO is entirely pyridyl ring localised then a quinoxaline vibration may be enhanced if the radical anion transition populates a MO with amplitude at the quinoxaline ring. The other possible mode of enhancement would be if the redox MO had amplitude on the quinoxaline ring itself. It is unlikely that the 1478 cm^{-1} band is a neutral quinoxaline mode because it shows no shift in wavenumber between $\mathbf{1}^-$ and $\mathbf{3}^-$. The quinoxaline mode for **1** and **3** lies at 1476 and 1470 cm^{-1} respectively. This suggests there is some amplitude of the redox MO on the quinoxaline ring. The fact that for $\mathbf{2}^-$ this band lies at 1487 cm^{-1} may be explained in terms of the reduced mass of the quinoxaline ring by removal of the pendant pyridyl.

There are a number of bands in the 1300 cm^{-1} region which show distinct signatures for the three reduced complexes. This suggests the redox MO has some amplitude on the quinoxaline ring.

The resonance-Raman data suggest that the redox MOs in complexes $\mathbf{1}^-$–$\mathbf{3}^-$ have significant pyridyl character with some contribution of the MO on the quinoxaline ring. The rather modest spectral differences between $\mathbf{1}^-$ and $\mathbf{2}^-$ suggest that the pendant pyridyl ring has little effect on the nature of the redox MO. This is consistent with the electrochemistry, which shows that **1** and **2** have equivalent $E^{\circ\prime}$ values, crystal structure, which shows the pendant pyridyl to be at 50° to the quinoxaline ring, and NMR data, which suggest the non-planarity of the rings are maintained in solution.

The resonance-Raman spectra for the excited states of complexes **1** and **3** are significant in that they show spectral signatures very like those of the corresponding $\mathbf{1}^-$ and $\mathbf{3}^-$ species. Close examination of the high-flux spectrum of **1** shows two distinct bands at 1597 and 1569 cm^{-1}. These correspond very closely to the 1604, 1586 and 1565 cm^{-1} bands of $\mathbf{1}^-$. The greater bandwidth of the 448 nm pulsed beam will correspondingly broaden the Raman scattering generated. Therefore the bands will be broadened out. This strongly suggests that the MLCT state, **1***, has a radical anion species almost identical in nature to that of $\mathbf{1}^-$. The excited-state resonance-Raman spectrum of **3** shows almost complete bleaching of ground-state features at 1335 and 1388 cm^{-1} at the highest flux density. This suggests that the high-pulse power spectrum is almost all excited state. This shows features at 1569 and 1473 cm^{-1} which closely correspond to $\mathbf{3}^-$ bands. The experiments on **1** and **3** were carried out with the same pulse energies and absorbed photon : molecule ratios. The observation of greater ground-state depletion in **3** than **1** would suggest the excited-state lifetime of **3** is the longer of the two. This would be consistent with the higher energy gap for **3**. The blue-shifting of the MLCT band and more negative $E^{\circ\prime}$ value for reduction is consistent with this.

Attempts to measure the excited-state lifetimes by emission techniques were unsuccessful due to low signal intensities. The fact that under pulsed excitation significant ground state is present suggests lifetimes of the order of 10 ns or less.

Conclusion

The following conclusions may be made from this study.

(1) The differing ligands have little effect on the electrochemical and infrared properties of the complexes.

(2) Crystal structure studies reveal that the unbound pyridine unit in complex **1** is not planar with the quinoxaline ring. Furthermore the NMR spectra suggest this non-planarity is retained in solution.

(3) Changes in the electronic spectra on reducing the mononuclear complexes show that all of the reduced species absorb at 470 nm. This signature is unlike that for $\mathbf{4}^-$, suggesting differences between the redox MOs for each.

(4) Comparison of the resonance-Raman spectra of complexes $\mathbf{1}^-$ and $\mathbf{4}^-$ confirms conclusion (3). The spectral signature for $\mathbf{4}^-$ shows no bands that can be related to the quinoxaline ring system. The spectrum of $\mathbf{1}^-$ shows a band at 1478 cm^{-1} which is quinoxaline-based. This suggests that the redox MO in $\mathbf{1}^-$ is spread over the pyridyl and quinoxaline rings.

(5) Spectral comparison of species $\mathbf{1}^-$–$\mathbf{3}^-$ suggests that the high-wavenumber modes, which are common to all three systems, are associated with the bound pyridyl ring.

(6) The excited-state resonance-Raman spectra of complexes **1** and **3** show that the MLCT excited states are very similar to the reduced complexes. This suggests the use of spectroelectrochemistry to model the excited state is a valid approach.

(7) The features for species $\mathbf{1}^-$–$\mathbf{3}^-$ provide spectral marker bands for the radical anions of the ligands pq, dpq and mdpq. Analysis of the previously studied $[Ru(bpy)_2L]^{2+}$ complexes reveal that no radical anion features are present in the resonance-Raman spectra of the reduced complexes, even as weak features. We are currently studying ruthenium(II) complexes in which the 2,2′-bipyridine ligand is replaced by a different bidentate polypyridyl ligand which retains the electronic properties of bpy but has a much lower scattering cross-section.

Acknowledgements

Support from the New Zealand Lottery Commission and the University of Otago Research Committee for the purchase of the Raman spectrometer is gratefully acknowledged. M. R. W. thanks the John Edmond postgraduate scholarship and Shirtcliffe fellowship for support for Ph.D. research. We also thank the University of Otago Chemistry Department for the award of a Ph.D. scholarship (to T. J. S.). We wish to thank the Massey University Research Fund for funding toward crystallographic data collection. This work was supported, in part, by the New Zealand Public Good Science Fund (Contract number UOO-508).

References

1 F. Scandola, R. Argazzi, C. A. Bignozzi, C. Chiorboli, M. T. Indelli and M. A. Rampi, in *Supramolecular Chemistry*, eds. V. Balzani and L. DeCola, Kluwer, Dordrecht, 1992; S. Roffia, M. Marcaccio, C. Paradisi, F. Paolucci, V. Balzani, G. Denti, S. Serroni and S. Campagna, *Inorg. Chem.*, 1993, **32**, 3003; K. Kalyanasundaram and Md. K. Nazeeruddin, *Inorg. Chim. Acta*, 1994, **226**, 213.
2 T. J. Simpson and K. C. Gordon, *Inorg. Chem.*, 1995, **34**, 6323.
3 F. Scandola, M.T. Indelli, C. Chiorboli and C. A. Bignozzi, *Top. Curr. Chem.*, 1990, **158**, 73.
4 V. Balzani, A. Juris, M. Venturi, S. Campagna and S. Serroni, *Chem. Rev.*, 1996, **96**, 759 and refs. therein.
5 J. B. Cooper, D. B. MacQueen, J. D. Petersen and D. W. Wertz, *Inorg. Chem.*, 1990, **29**, 3701.
6 H. A. Goodwin and F. Lions, *J. Am. Chem. Soc.*, 1959, **81**, 6415.
7 N. Hadjiladis, S. Kasselouri, A. Garoufis, A. Kakhariakis, G. Kalkanis and S. P. Perlepes, *Inorg. Chim. Acta*, 1993, **207**, 255.
8 D. P. Strommen and K. Nakamoto, *Laboratory Raman Spectroscopy*, Wiley, New York, 1984.
9 P. C. Lee and D. Miesel, *J. Phys. Chem.*, 1982, **86**, 3391.
10 A. Babaei, P. A. Connor, A. J. McQuillan and S. Umapathy, *J. Chem. Educ.*, 1997, **74**, 1200.
11 C. A. Grant and J. L. Hardwick, *J. Chem. Educ.*, 1997, **74**, 318.
12 SDP, Structure Determination Package, Enraf-Nonius, Delft, 1985.
13 G. M. Sheldrick, SHELXL 93, Institut für Anorganische Chemie der Universität Göttingen, 1993.
14 D. R. Gamelin, M. W. George, P. Glyn, F.-W. Grevels, F. P. A. Johnson, W. Klotzbucher, S. L. Morrison, G. Russell, K. Schaffner and J. J. Turner, *Inorg. Chem.*, 1994, **33**, 3246.

15 M. W. George, F. P. A. Johnson, J. R. Westwell, P. M. Hodges and J. J. Turner, *J. Chem. Soc.*, *Dalton Trans.*, 1993, 2977.
16 A. Juris, S. Campagna, I. Bidd, J.-M. Lehn and R. Ziessel, *Inorg. Chem.*, 1988, **27**, 4007.
17 R. Lin, T. F. Guarr and R. Duesing, *Inorg. Chem.*, 1990, **29**, 4169.
18 R. J. H. Clark and T. J. Dines, *Angew. Chem.*, *Int. Ed. Engl.*, 1986, **25**, 131.
19 M. Flieschmann, P. M. Hendra and A. J. McQuillan, *J. Chem. Soc.*, *Chem. Commun.*, 1973, 80.
20 T. Shida, *Electronic Absorption Spectra of Radical Ions*, Elsevier, Amsterdam, 1988.
21 K. C. Gordon and J. J. McGarvey, *Chem. Phys. Lett.*, 1989, **162**, 117.
22 C. K. Johnson, ORTEP, Report ORNL-5138, Oak Ridge National Laboratory, Oak Ridge, TN, 1976.
23 (*a*) E. W. Abel, V. S. Dimitrov, N. J. Long, K. G. Orrell, A. G. Osborne, H. M. Pain, V. Sik, M. B. Hursthouse and M. A. Mazid, *J. Chem. Soc.*, *Dalton Trans.*, 1993, 597; (*b*) D. A. Bardwell, F. Barigelletti, R. L. Cleary, L. Flamigni, M. Guardigli, J. C. Jeffery and M. D. Ward, *Inorg. Chem.*, 1995, **34**, 2438; (*c*) P. Chen, M. Curry and T. J. Meyer, *Inorg. Chem.*, 1989, **28**, 2271; (*d*) J. Guilhem, C. Pascard, J.-M. Lehn and R. Ziessel, *J. Chem. Soc.*, *Dalton Trans.*, 1989, 1449; (*e*) L. E. Helberg, J. Barrera, M. Sabat and W. D. Harman, *Inorg. Chem.*, 1995, **34**, 2033; (*f*) N. M. Iha and G. J. Ferraudi, *J. Chem. Soc.*, *Dalton Trans.*, 1994, 2565; (*g*) R. Lin, Y. Fu, C. P. Brock and T. F. Guarr, *Inorg. Chem.*, 1992, **31**, 4346; (*h*) S. A. Moya, J. Guerrero, R. Pastene, R. Schmidt, R. Sariego, R. Sartori, J. Sanz-Aparicio, I. Fonseca and M. Martínez-Ripoll, *Inorg. Chem.*, 1994, **33**, 2341; (*i*) J. Rall, F. Weingart, D. M. Ho, M. J. Heeg, F. Tisato and E. Deutsch, *Inorg. Chem.*, 1994, **33**, 3442; (*j*) R. J. Shaver, M. W. Perkovic, D. P. Rillema and W. Clifton, *Inorg. Chem.*, 1995, **34**, 5446; (*k*) M. Stebler, A. Gutiérrez, A. Ludi and H.-B. Bürgi, *Inorg. Chem.*, 1987, **26**, 1449; (*l*) W. Tikkanen, W. C. Kaska, S. Moya, T. Laymn and R. Kane, *Inorg. Chim. Acta*, 1983, **76**, L29; (*m*) V. W. -W. Yam, K. K.-W. Lo, K.-K. Cheung and R. Y.-C. Kong, *J. Chem. Soc.*, *Chem. Commun.*, 1995, 1191; (*n*) V. W.-W. Yam, V. C.-Y Lau and K.-K. Cheung, *J. Chem. Soc.*, *Chem. Commun.*, 1995, 259; (*o*) V. W.-W. Yam, K. M.-C. Wong, V. W.-M. Lee, K. K.-W. Lo and K.-K. Cheung, *Organometallics*, 1995, **14**, 4034; (*p*) A. Escuer, R. Vicente, T. Comas, J. Ribas, M. Gomez, X. Solans, D. Gatteschi and C. Zanchini, *Inorg. Chim. Acta*, 1991, **181**, 51; (*q*) D. P. Rillema, D. G. Taghdiri, D. S. Jones, C. D. Keller, L. A. Worl, T. J. Meyer and H. A. Levy, *Inorg. Chem.*, 1987, **26**, 578; (*r*) S. C. Rasmussen, M. M. Richter, E. Yi, H. Place and K. J. Bewer, *Inorg. Chem.*, 1990, **29**, 3926.
24 S. Van Wallendael, R. J. Shaver, D. P. Rillema, B. J. Yoblinski, M. Stathis and T. F. Guarr, *Inorg. Chem.*, 1990, **29**, 1761.
25 M. Maruyama, H. Matsuzawa and Y. Kaizu, *Inorg. Chim. Acta*, 1995, **237**, 159.
26 C. H. Braunstein, D. A. Baker, T. C. Strekas and H. D. Gafney *Inorg. Chem.*, 1984, **23**, 857.
27 M. M. Richter and K. J. Brewer, *Inorg. Chem.*, 1990, **29**, 3926.
28 D. P. Strommen, P. K. Mallick, G. D. Danzer, R. S. Lumpkin and J. R. Kincaid, *J. Phys. Chem.*, 1990, **94**, 1357.
29 J. B. Cooper, D. B. McQueen, J. D. Petersen and D. W. Wertz, *Inorg. Chem.*, 1990, **29**, 3701.
30 F. R. Dollish, W. G. Fateley and F. F. Bentley, *Characteristic Raman Frequencies of Organic Compounds*, Wiley, New York, 1974.
31 K. C. Gordon, A. H. R. Al-Obaidi, P. M. Jayaweera, J. J. McGarvey, J. F. Malone and S. E. J. Bell, *J. Chem. Soc.*, *Dalton Trans.*, 1996, 1591.
32 M. W. George, F. P. A. Johnson, J. J. Turner and J. R. Westwell, *J. Chem. Soc.*, *Dalton Trans.*, 1995, 2711.

Received 21*st July* 1997; *Paper* 7/05194H